Published in final edited form as:
Clin Cancer Res. 2014 September 1; 20(17): 4636–4646. doi:10.1158/1078-0432.CCR-14-0305.

miR-409-3p/-5p promotes tumorigenesis, epithelial to mesenchymal transition and bone metastasis of human prostate cancer

Sajni Josson[1,*], **Murali Gururajan**[1,*], **Peizhen Hu**[1], **Chen Shao**[1], **Gina Chia-Yi Chu**[1], **Haiyen E. Zhau**[1], **Chunyan Liu**[1], **Kaiqin Lao**[2], **Chia-Lun Lu**[1], **Yi-Tsung Lu**[1], **Jake Lichterman**[1], **Srinivas Nandana**[1], **Quanlin Li**[3], **Andre Rogatko**[3], **Dror Berel**[3], **Edwin M. Posadas**[1], **Ladan Fazli**[4], **Dhruv Sareen**[5], and **Leland W. K. Chung**[1]

[1]Uro-Oncology Research Program, Department of Medicine, Samuel Oschin Comprehensive Cancer Institute, Cedars-Sinai Medical Center, Los Angeles, USA

[2]Genetic Systems, Life Technologies Inc., South San Francisco, California, USA

[3]Department of Biostatistics and Bioinformatics, Samuel Oschin Comprehensive Cancer Institute, Cedars-Sinai Medical Center, Los Angeles, USA

[5]Regenerative Medicine Institute, Cedars-Sinai Medical Center, Los Angeles, USA

[4]Vancouver Prostate Cancer Center, University of British Columbia, Vancouver, Canada

Abstract

Purpose—miR-409-3p/-5p is a microRNA expressed by embryonic stem cells and its role in cancer biology and metastasis is unknown. Our pilot studies demonstrated elevated miR-409-3p/-5p expression in human prostate cancer bone metastatic cell lines, therefore we defined the biological impact of manipulation of miR-409-3p/-5p in prostate cancer progression and correlated the levels of its expression with clinical human prostate cancer bone metastatic specimens.

Experimental Design—miRNA profiling of prostate cancer bone metastatic EMT cell line model was performed. Gleason score human tissue array was probed for validation of specific miRNAs. Additionally, genetic manipulation of miR-409-3p/-5p was performed to determine its role in tumor growth, epithelial to mesenchymal transition (EMT) and bone metastasis in mouse models.

Results—Elevated expression of miR-409-3p/-5p was observed in bone metastatic prostate cancer cell lines and human prostate cancer tissues with higher Gleason scores. Elevated miR-409-3p expression levels correlated with prostate cancer patient progression free survival. Orthotopic delivery of miR-409-3p/-5p in the murine prostate gland induced tumors where the tumors expressed, EMT and stemness markers. Intracardiac inoculation (to mimic systemic dissemination) of miR-409-5p inhibitor treated bone metastatic $ARCaP_M$ prostate cancer cells in

Corresponding co-authors: Murali Gururajan, Sajni Josson or Leland Chung, Uro-Oncology Research Program, Department of Medicine, Samuel Oschin Comprehensive Cancer Institute, Cedars-Sinai Medical Center, Los Angeles, CA. 90048., Phone: 310-423-7622 ; Fax: 310-423-8543., Murali.Gururajan@cshs.org, Sajni.Josson@cshs.org, Leland.Chung@cshs.org.
*These authors contributed equally to the manuscript.

mice, led to decreased bone metastasis and increased survival compared to control vehicle-treated cells.

Conclusion—miR-409-3p/-5p plays an important role in prostate cancer biology by facilitating tumor growth, EMT and bone metastasis. This finding bear's particular translational importance since miR-409-3p/-5p appears to be an attractive biomarker and/or possibly a therapeutic target to treat bones metastatic prostate cancer.

Keywords

miR-409; DLK1-DIO3 cluster; prostate cancer bone metastasis

INTRODUCTION

Metastasis of cancer cells to distant organs involves EMT, an embryonic process hijacked by the cancer cells. The role of noncoding RNAs in both the EMT and subsequent bony metastasis is less well-understood. Recent studies highlight the role of noncoding RNAs including microRNAs and lncRNAs in cancer progression and metastasis (1–5). The delta-like 1 homolog- deiodinase, iodothyronine 3 (DLK1-DIO3) imprinted embryonically cluster contains several large and small noncoding RNA genes, which are deregulated in cancer development (6, 7). The DLK1-DIO3 gene cluster was previously shown to be aberrantly silenced in human and mouse induced pluripotent stem cells (iPSCs) but not in fully pluripotent embryonic stem cells, indicating the importance in the generation of fully functional iPSCs (8, 9). This suggests that certain miRNAs in this region are involved in totipotency. Several studies show that some miRNAs in this cluster are differentially expressed in prostate, breast and liver cancer (7, 10, 11). Interestingly, miRNA members of the DLK1-DIO3 cluster have been shown to be upregulated in the serum of cancer patients. Specifically, in prostate cancer (PCa), miR-409-3p has been shown to be upregulated in the serum of high risk PCa patients compared to low risk PCa patients (12). miR-379 expression was increased in the tissues of metastatic PCa compared to localized PCa (13). Also, miR-379 and miR-154* have been shown to be increased in circulating exosomes of patients with lung adenocarcinomas versus healthy smokers (14). In this study, we manipulated miR-409-3p/-5p expression in adult normal prostate and in PCa cells and report a surprising and novel discovery of transforming effects of this miRNA conferring prostate epithelium to undergo EMT, and expressing stemness and tumorigenic phenotypes in mice. Inhibition of miR-409-5p in a human PCa cell line resulted in decreased bone metastasis *in vivo.*

MATERIALS AND METHODS

Cell culture

Human androgen-refractory PCa $ARCaP_E$ and $ARCaP_M$ and LNCaP, $LNCaP^{Neo}$ and $LNCaP^{RANKL}$ PCa (15–17) were used. PCa cells and 293T cells were cultured in T-medium (GibcoBRL) supplemented with 5% heat inactivated fetal bovine serum (Bio-Whittaker) as previously mentioned (18). All cells were tested for mycoplasma every three months and were negative. The embryonic stem cells and iPSCs derived small RNA preparations were

provided by Drs. Sareen and Svendsen. Derivation of these cells is included in the Supplementary materials and methods and figure legends.

miRNA expression

Quantitative Real Time PCR (qRT-PCR)—miRNA expression analysis by qRT-PCR was performed separately for each miRNA using specific primer sets (Applied Biosystems) as previously described (19). RNU6B was used for normalization.

mRNA analysis—Total RNA was isolated using the RNeasy Mini Kit (Qiagen). cDNA was made using Superscript®III reverse transcriptase (Life Technologies). mRNA primers were designed and synthesized at Integrated DNA Technologies. mRNA expression levels were determined by qRT-PCR assays and SYBR Green Dye (Applied Biosystems).

Long noncoding RNA analysis

mRNA was extracted as described above. LncRNA expression levels were determined as per manufacturer's instruction (System Biosciences) using real-time PCR. Relative levels of MEG9 were plotted normalized to GAPDH.

Cytoscape analysis

Cytoscape image was created using miR-409-5p and miR-409-3p target genes from Targetscan v12 software analysis and Genecard website (STRING: functional protein association networks).

In situ hybridization (ISH)-Quantum dots (QD)

Human Gleason Tissue array—A Gleason score tissue array was obtained from Vancouver Prostate Center. The use of specimens in research was approved by the institution review board of the Cedars-Sinai Medical Center (IRB# Pro21228). The tissues consisted of benign prostatic hyperplasia (BPH) (N=14), Gleason 6 (N=26) and Gleason ≥7 (N=35). Each tissues had two cores in the array. These patients had no treatment. The tissue array was stained for H&E and graded by a pathologist. Information on Gleason score of the cancer and miR-409 intensity is included in Supplementary Fig. S1. The control scramble and miR-409-5p and -3p probes were 5′-biotin labeled. The probes were linked to streptavidin-conjugated QD. Multiplex QD labeling (mQDL) was performed as previously described (16). miR-409-5p was labelled with 625 nm QD (red) followed by miR-409-3p (green) which was labeled with 565 nm QD (16). The QD fluorescence intensity of each tissue section was determined and analyzed. Statistical analysis was performed on the data set using a Kruskal-Wallis one way analysis of variance and post hoc Tukey method for multiple comparisons between groups. Data distribution was depicted as box plots.

***In vivo* animal studies—**Mouse tumor and tumor xenografts were formalin-fixed and paraffin-embedded. miRNA ISH protocol was followed as per manufacturer's instruction (Exiqon, MA). Single QD labeling was performed as previously mentioned (16). Scramble, miR-409-5p or miR-409-3p probes were labeled with 625 nm QDs (16). Images were taken at 40x. H&E staining was performed on subsequent tissue sections.

MSKCC dataset analysis

The dataset was published by MSKCC team (20) and was obtained from cBioPortal (21). miR-409-3p but not miR-409-5p was analyzed in the dataset. For the analysis of miR-409-3p with different Gleason scores, patients with Gleason score 6 or 7 (n=86) were grouped together to compare with those with Gleason score 8 or 9 (n=12). Student t test was done between the two groups for analysis of differential expression of miR-409-3p between two cohorts. For the survival analysis, the expression levels of miR-409-3p in patients were compared with the median expression level of normal individuals. The disease free survival of patients with miR-409-3p expression levels higher than normal individual (n=29) was compared with that with lower miR-409-3p expression levels (n=78). Kaplan-Meier survival curve was done by log-rank test between high and low expression groups.

Lentiviral transduction

$ARCaP_E$ or LNCaP PCa cell lines were transduced with miR-409 lentivirus expressing green fluorescent protein (GFP) or control GFP lentivirus and $ARCaP_M$ PCa cell lines were transduced with miR-409-5p lentivirus expressing GFP or control GFP lentivirus. Lentiviral preparation and transduction of cell lines were performed as per the manufacturer's instructions (System Biosciences). GFP positive cells were FACS sorted and cultured *in vitro*.

Growth assay, invasion and migration assays

$ARCaP_M$-C and $ARCaP_M$-409-5pi cells were grown and counted for a week. Cell viability assay was performed using MTS assay as previously mentioned (18). Cancer cell invasion and migration were assayed in Companion 24-well plates (Becton Dickinson Labware) as described previously (22).

Western Analysis

Western analysis was performed as previously described (22). The membranes were incubated with mouse monoclonal antibody against STAG2 (Cell Signaling technology), RSU1 (Proteintech Group), β-actin (Sigma-Aldrich) respectively, at 4 °C overnight.

Xenograft studies

All animal experiments were IACUC approved and done in accordance with institutional guidelines.

Orthotopic study—Preparation of grafts: 293T cells were transduced with either miR-409 expressing lentiviral vector carrying GFP or control vector carrying a GFP plasmid (System Biosciences) viral particles. 293T cells were incubated for 24 h and the cells were trypsinized. Cell grafts were made by mixing 3 parts of rat tail collagen and 1.2 parts of setting solution. The mixture was added to the 293T cells. The mixture (6×10^5 293T cells) was orthotopically injected into four-week-old male nude mice (NCRNU, Taconic) prostates (N=5/group). The control or miR-409 GFP plasmids were expected to be released from the 293T cells and enter the adjacent epithelium and stroma of the mouse prostate. The 293T cells were lysed when the viruses were released. Mice were monitored for miR-409

expression by detecting GFP fluorescence and for tumor growth using NIR dye (IR783) (23) using IVIS® Lumina Imaging system. Tumors developed from 2–6 months in the miR-409 group. Mice were euthanized and tumors sections were stained for specific markers.

Immunohistochemistry (IHC)

IHC staining was performed as previously described (22). The following primary antibodies were used: Ki-67 (Abcam), STAG2, p-AKT (Cell Signaling technologies), RSU1 (Proteintech Group), Vimentin (V9), Nanog, Oct-3/4, cytokeratin 5 (Santa Cruz Biotechnology), cytokeratin 8 (Covance, Inc.) were used. Additional information attached in the Supplementary materials and methods and figure legends.

***In vivo* metastasis study—**Luciferase tagged $ARCaP_M$ control and $ARCaP_M$-409-5pi cells were injected intra-cardially as previously mentioned (24) in male SCID/beige mice (Charles River Laboratories) (N=5/group). Mice were imaged for bioluminescence and X-ray detection using IVIS® Lumina Imaging system. Mice were euthanized when they produced large tumors. Mice were given NIR dye (IR783) 48 h before euthanasia, the tumor specific NIR dye was used to detect metastatic tumor in the mice.

Statistical analysis

Values were expressed as means ± standard deviation. All experiments were done in triplicates at least two independent times. Statistical analysis was performed using Student's t-test. For tissue Gleason score array, the difference between the groups were tested by Kruskal-Wallis one way analysis of variance. A post hoc Tukey method was used to enable multiple comparisons between groups. Values of $p<0.05$ were considered to be statistically significant.

RESULTS

MicroRNA miR-409-3p/-5p is overexpressed in bone metastatic EMT models of human PCa

To understand the regulatory role of microRNAs in EMT and PCa bone metastasis, we performed miRNA profiling of two lineage-related, differentially bone metastatic human PCa cell lines, $ARCaP_E$ (non-metastatic line) and $ARCaP_M$ (metastatic line), denoted respectively their epithelial ($ARCaP_E$) and mesenchymal ($ARCaP_M$) phenotype (15, 25) (Supplementary Table. S2, S3). The differential miRNA expression of the non-metastatic ($ARCaP_E$) and metastatic PCa cells ($ARCaP_M$) are represented in a Supplementary Table S3. We observed markedly upregulated miR-409-3p/-5p expression in the bone metastatic $ARCaP_M$ variant (Fig. 1A). miR-409-3p and-5p miRNAs were in the top five of the differentially expressed miRNAs between $ARCaP_M$ and $ARCaP_E$ PCa cells. We observed a similar increases in miR-409-5p/-3p expression in the $LNCaP^{Neo}$ verses $LNCaP^{RANKL}$ (16, 17) bone metastasis PCa model (Fig. 1A). Thus, in two different PCa bone metastatic EMT models, we observed an increase in miR-409-5p/-3p. miR-409-3p and -5p are generated from an immature transcript and transcribed from the 5′ end of the pre-miRNA. miR-409 is located in a region that overlaps the long non-coding RNA MEG9 (26). The expression levels of MEG9 lncRNAs hence were elevated in the metastatic $ARCaP_M$ PCa cells compared to non-metastatic $ARCaP_E$ PCa cells (Fig. 1B). In addition to bone metastatic

human PCa cells, human embryonic stem cells and induced pluripotent cells also notably expressed elevated levels of miR-409-3p/-5p (Fig. 1C, 1D). Thus, we demonstrate that miR-409-3p/-5p is upregulated in two aggressive, bone metastatic EMT PCa models and in human embryonic stem cells and iPSCs.

miR-409-3p/-5p inhibits tumor suppressor genes in PCa

Targetscan 6.2 (June 2012) software analysis revealed putative miR-409-5p targets that include tumor suppressor genes like stromal antigen 2 (STAG2), ras suppressor protein 1 (RSU1), retinoblastoma-like 2 (RBL2) and nitrogen permease regulator-like 2 (NPRL2). Predicted mRNA targets of miR-409-3p include polyhometic 3 (PHC3), RSU1 and tumor suppressor candidate 1 (TUSC1). The miR-409-5p and -3p targets were validated by qRT-PCR and were found to be downregulated in metastatic $ARCaP_M$ cells that express elevated levels of miR-409-3p/5p compared to $ARCaP_E$ cells that express lower levels of miR-409-3p/5p (Fig. 2A). Consistently we observed elevated protein expression of STAG2 and RSU1 in $ARCaP_E$ cells compared to $ARCaP_M$ cells (Fig. 2B). We demonstrated that miR-409-5p binds the 3′UTR of STAG2 and RSU1 (Supplementary Fig. S4B, C). Additionally the binding sites of miR-409-5p and miR-409-3p on RSU1 3′UTR are indicated in Supplementary Fig. S4A. Using gene cards and string interactions, we created a cytoscape map of the possible human cancer pathways regulated by miR-409-5p and miR-409-3p that would account for its activity in cells. miR-409-3p is predicted to activate the Ras signaling pathway, hypoxia inducible factor-1α pathway, regulate polycomb group proteins and osteoblastic pathways (Fig. 2C). miR-409-5p is predicted to activate E2F pathway, Ras signaling pathway, Akt pathway and aneuploidy (Fig. 2D). Taken together, we demonstrate that miR-409-3p/-5p is elevated in the bone metastatic EMT cell models and it functions by repressing several tumor suppressor genes.

Human prostatic tissues with higher Gleason score and prostate cancer bone metastasis tissues express elevated levels of miR-409

In order to validate our findings in clinical samples, we determined the levels of miR-409-3p/-5p in human prostate tissues with various Gleason scores using *in situ* hybridization (ISH) and multiplexed quantum dot (QD) labeling. The miRNA probes were biotin-labeled (Exiqon) and further labeled to a streptavidin conjugated QD at a specified wavelength. miR-409-3p/-5p was detected both in the tumor tissues. The tissues were separated into three groups, BPH (N=14), Gleason 6 (N=26) and Gleason ≥7 (N=35). Tumors with higher Gleason ≥7 had significantly higher miR-409-3p and miR-409-5p staining in the tumor areas compared to the tissues with BPH. miR-409-3p was significantly higher in the Gleason ≥7 compared to Gleason 6 (Fig. 3A), as analyzed by Kruskal-Wallis one way analysis of variance- Tukey method. A representative image of Gleason 8, shows increased staining of miR-409-3p (green) and -5p (red) in PCa tissues (Fig. 3B). We used a dataset published by MSKCC (20) to determine the miR-409-3p expression in different Gleason score tissues in Fig 3C. The miR-409-3p expression levels were compared between Gleason_low (Gleason 6,7 ; n=86) and Gleason_high (Gleason 8, 9; n=12) groups (Fig. 3C). miR-409-3p expression was significantly elevated in higher Gleason tissues compared to low Gleason tissues, consistent with our own staining data (p value = 0.0151). The miR-409-5p expression was not provided in this dataset. Furthermore, we analyzed the

survival of this patient cohort based on their miR-409-3p expression level (Fig. 3D). The patients were separated into two groups based on their miR-409-3p expression levels relative to the normal samples. We found that the patients with higher miR-409-3p than normal sample were correlated with poor progression free survival ($p=4.32 \times 10^{-5}$). This suggests the miR-409-3p is clinically relevant in PCa. Collectively, these results demonstrate that miR-409 expression correlated with higher Gleason score in prostatic tissues and with patient progression free survival, possibly linking miR-409 expression with tumor progression.

Ectopic expression of miR-409-3p/-5p leads to increased invasiveness and aggressiveness of PCa cells and conversely inhibition of miR-409-3p/-5p results in increased cell death in PCa cells

To determine the effects of miR-409-3p/-5p action in PCa, we ectopically introduced this miRNA in less aggressive epithelial-type $ARCaP_E$ cells and LNCaP cells. A significant increase in miR-409-3p/-5p expression was confirmed using qRT-PCR (Fig 4A, Supplementary Fig. 5A). The mRNA expression of target genes of miR-409-3p/-5p was determined using qRT-PCR. We report that miR-409-5p target mRNAs (STAG2, RSU1, RBL2, and NPRL2) were decreased in $ARCaP_E$ cells that overexpress miR-409 ($ARCAP_E$-409) compared to the control miRNA-treated cells (Fig. 4B). Two of the three mRNA targets of miR-409-3p were also decreased in $ARCaP_E$-409 cells compared to control (RSU1 and TUSC1), but not PHC3 (Fig. 4B). Moreover, $ARCaP_E$-409 cells showed increased migratory and invasive capacity compared to control PCa cells (Fig 4C).

On the contrary, inhibition of miR-409-3p in $ARCaP_M$ PCa cells using a shRNA inhibitor resulted in cell death of PCa cells and hence further experiments could not be carried out due to complete lethality of the cells *in vitro*. Inhibition of miR-409-5p using shRNA resulted in cell death of aggressive metastatic PCa cells (Fig. 4D) compared to the control scramble miRNA expressing cells. We generated stable lentiviral clones of $ARCaP_M$ PCa cells expressing miR-409-5p inhibitor ($ARCaP_M$-409-5pi). $ARCaP_M$-409-5pi PCa cells had a decreased growth rate compared to $ARCaP_M$-C cells (Fig. 4D). $ARCaP_M$-409-5pi cells had decreased miR-409-5p levels compared to $ARCaP_M$-C cells (Fig. 4E). Next, we measured the levels of mRNA targets of miR-409-5p, which include NPRL2 and STAG2, and found that they were increased in $ARCaP_M$-409-5pi treated cells compared to $ARCaP_M$-C control cells (Fig 4F). Furthermore, immunoblot analysis confirmed increases in protein levels of STAG2 and RSU1 in $ARCaP_M$-409-5pi cells compared to control cells (Fig. 4G). Taken together, these results demonstrate that over-expression of miR-409-3p/-5p in less aggressive PCa cells decreased their expression of tumor suppressors and increased their invasion and migration whereas inhibition of miR-409-5p in aggressive PCa cells decreased their growth and increased their cell death.

Ectopic expression of miR-409-3p/-5p in the prostate gland transforms normal prostate epithelia, promotes tumorigenecity, EMT and stemness *in vivo*

To test if miR-409-3p/-5p is oncogenic *in vivo*, we implanted human embryonic kidney cells, 293T producer cells, transfected with the miR-409 expressing lentiviral vector carrying green fluorescent protein (GFP) or control vector carrying a GFP plasmid,

orthotopically into the prostate gland of athymic nude mice (N = 5/group). Tumor development was monitored using the tumor specific near- infrared (NIR) dye (IR783) (23). The rationale behind this procedure is that the lentivirus will be secreted by the producer cells (293T) and infect prostate epithelial and/or stromal cells *in vivo*. Strikingly, prostate tumors developed in two to five months in three out of five mice that received the producer cells transfected with miR-409 (Fig. 5A). Mice that were implanted with producer cells expressing control lentiviral plasmid did not develop any tumors in the prostate. The tumors had green fluorescence and showed tumor specific dye uptake (IR783) (Fig. 5A). H&E staining of tissue sections revealed tumors ranging from prostatic interstitial neoplasia, basal cell hyperplasia, and adenocarcinoma in the miR-409 prostates (Fig. 5B). The tissue sections were also analyzed for miR-409-3p/-5p levels using ISH-QD labeling. miR-409-3p and miR-409-5p expression was observed only in miR-409 expressing prostates in tumor cells but not in control prostates (Fig. 5B). Levels of miR-409 expression appear to correlate with the overall size of the tumors. Immunohistochemical staining revealed elevated expression of tumor proliferation markers such as Ki-67 and oncogenic kinases like p-AKT (Fig. 5C), downregulated expression of STAG2 and RSU1 and upregulated expression of mesenchymal markers, such as vimentin, when compared to the control prostate gland (Fig. 5C). Immunohistochemical staining of orthotopic tumors revealed positive staining of Oct-3/4 (strong nuclear staining) and Nanog (weak nuclear staining), both of which are stem cell markers, in both the epithelial and the stromal compartment of miR-409 expressing neoplastic prostates (Supplementary Fig. S6). Strikingly, in the epithelial compartment, both the basal and luminal cells in the prostate underwent proliferation, as exhibited by strong Ki-67 staining, in response to uptake of miR-409-3p/-5p, with cytokeratin 5, representing the basal cell marker and cytokeratin 8, representing the luminal cell marker (Supplementary Fig. S6). Taken together, these studies suggest that, miR-409-3p/-5p is oncogenic and its expression is sufficient to drive tumorigenesis of the adult normal prostate gland.

Inhibition of miR-409-5p results in decreased bone metastasis of aggressive PCa *in vivo*

Since inhibition of miR-409-3p using a shRNA inhibitor resulted in complete cell lethality, further experiments could not be carried out. Inhibition of miR-409-5p in $ARCaP_M$ cells resulted in reversal of EMT (MET; Fig. 6A), accompanied by an increase in E-cadherin expression and a decrease in N-cadherin expression and epithelial morphological changes (Fig. 6A). Inversely, overexpression of miR-409 in $ARCaP_E$ and LNCaP resulted in decreased E-cadherin expression (Supplemental Fig. S5C). Knocking down miR-409-5p also resulted in moderate decrease in migration and invasion of cancer cells (Fig. 6A). To determine if miR-409 plays a role in cancer metastasis, we inoculated viable $ARCaP_M$-C control cells or viable $ARCaP_M$-409-5pi cells via the intracardiac route into SCID/Beige mice (N=5/group) to mimic *in vivo* metastasis. Mice that received $ARCaP_M$-C cells had 100% incidence of bone metastasis, whereas mice that received $ARCaP_M$-409-5pi cells did not develop any metastasis at 15 weeks. The luciferase tagged cancer cells were imaged by luciferase imaging (Fig. 6B). The survival of the $ARCaP_M$-C and $ARCaP_M$-409-5pi injected mice are depicted as a Kaplan Meier curve, where majority (4/5) of control mice died by 15 weeks but not $ARCaP_M$-409-5pi injected mice (Fig. 6C). Using X-ray imaging we observed bone metastatic tumor sites in tibia, femur, mandible and humerus (Fig. 6D). Each mouse developed 1 to 5 metastatic tumors in the control group, detected by IR783 imaging and

confirmed by luciferase imaging (Fig 6E). X-ray imaging of mice inoculated with $ARCaP_M$-409-5pi revealed no evidence of bone lesions consistent with the lack of luciferase signals (Fig. 6B and data not shown). Thus, inhibition of miR-409-5p induced MET and significantly abrogates the metastatic potential of metastatic PCa cells *in vivo*. Taken together, these studies demonstrate that miR-409 is associated with bone metastasis of human PCa cells in mouse models.

DISCUSSION

To understand the biology of noncoding RNAs in EMT and cancer bone metastasis and to identify novel biomarkers and/or therapeutic targets, we profiled miRNAs in unique EMT models of human PCa, developed in our laboratory. miR-409-3p/-5p, located within the DLK1-DIO3 cluster was highly upregulated in two PCa cell lines with mesenchymal phenotype and with bone metastatic potential (Fig. 1). The miRNA members of the DLK1-DIO3 cluster has been shown to be important for totipotency during embryogenesis and induced pluripotent stem cell formation. We report an unexpected discovery of the oncogenic role of miR-409-3p/-5p, which is expressed by embryonic stem cells and pluripotent stem cells, to promote PCa development and metastasis. Specifically, we showed that miR-409-3p/-5p: 1) is elevated in human PCa tumor tissues and correlates with PCa patients progression free survival, 2) can transform normal mouse prostate epithelium to exhibit tumorigenic phenotype and promote the growth and invasion of human PCa cells by downregulating tumor suppressor genes *in vitro* and *in vivo*, 2) can promote EMT and stemness of prostate epithelium *in vivo*, and 3) inhibition of miR-409-5p results in decreased bone metastatic tumor growth and increase in survival. Thus, miR-409 appears to be a promising new biomarker for cancer detection and an attractive new therapeutic target for PCa treatment.

Since, inhibition of miR-409-3p resulted in cell lethality; further studies in future will require the use of inducible systems. miR-409 appears to mediate its tumorigenic effects through targeting of tumor suppressor genes (Fig. 2, 4, 5). One such target gene of miR-409-3p and -5p is RSU1. Previous studies have shown that RSU1 protein blocks the oncogenic Ras/MAPK pathway and integrin-linked kinase (ILK) pathway in PCa (27–29). Another, target gene for miR-409-5p appears to be STAG2. In the tumor cells, STAG2 is part of the cohesion complex, where deregulation of the members of the cohesion complex is thought to cause aneuploidy, cancer initiation and progression (30, 31). In addition to STAG2, miR-409-5p appears to target NPRL2, a tumor suppressor protein decreased in solid tumors (32–34). There are differences in the genes targeted by miR-409-3p and miR-409-5p. At the same time, they do share some similar targets. Thus, miR-409-3p and miR-409-5p could be considered as distinct miRNAs with some shared functions.

Orthotopic delivery of miR-409-3p/-5p in mouse prostate resulted in adenocarcinoma as well as prostatic hyperplasia. This dual phenotype could be attributed to difference in uptake of levels of miR-409-3p/-5p by the mouse prostate. miR-409-3p was found to be elevated in the serum of PCa patients with high Gleason score (12). Consistently, we found that the metastatic $ARCaP_M$ cells secrete higher levels of miR-409 and inhibition of miR-409-5p in these cells decreases this process (Supplementary Fig. S7). Our metastatic model involves

injection of cells into the blood stream and hence sites of tumor formation could be sites that permit tumor growth, and in our study it is the bone. Hence future studies will require implantation of ARCaP$_M$-409-5pi cells in the prostate and study their bone metastatic ability.

Our data suggests that miR-409-3p and -5p are elevated in the tumor tissues of PCa and can predict poor prognosis and prostate cancer patient progression free survival. It was also observed that miR-409-3p and miR-409-5p co-localized with higher Gleason score compared to low Gleason score (data not shown). Thus, both the miRNAs are active in more aggressive cancer and together induce tumorigenesis. Inhibition of miR-409-5p *in vitro* resulted in decreased growth and MET, and this was extended in the *in vivo* setting where miR-409-5pi cells did not grow, thus inhibiting the metastatic ability of highly aggressive bone metastatic PCa cells *in vivo* (Fig. 6).

In summary, our study demonstrates the oncogenic roles of miR-409-3p/-5p that is capable of promoting the malignant transformation of prostate epithelium in mice, including EMT, stemness and bone metastasis. Therefore, miR-409-3p/-5p may be a new biomarker and a therapeutic target for the treatment of PCa bone metastasis.

Supplementary Material

Refer to Web version on PubMed Central for supplementary material.

Acknowledgments

We would like to thank Dr. Clive Svendsen for providing the embryonic and iPSCs. Grant support from P01-CA98912, DAMD-17-03-02-0033 and RO1-CA122602 (L.W.K. Chung). We would like to thank Dr. Christopher L. Haga for helping with generation of mutant luciferase constructs.

References

1. Ma L, Teruya-Feldstein J, Weinberg RA. Tumour invasion and metastasis initiated by microRNA-10b in breast cancer. Nature. 2007; 449:682–8. [PubMed: 17898713]
2. Tavazoie SF, Alarcon C, Oskarsson T, Padua D, Wang Q, Bos PD, et al. Endogenous human microRNAs that suppress breast cancer metastasis. Nature. 2008; 451:147–52. [PubMed: 18185580]
3. Zhang Y, Yang P, Sun T, Li D, Xu X, Rui Y, et al. miR-126 and miR-126* repress recruitment of mesenchymal stem cells and inflammatory monocytes to inhibit breast cancer metastasis. Nat Cell Biol. 2013; 15:284–94. [PubMed: 23396050]
4. Korpal M, Ell BJ, Buffa FM, Ibrahim T, Blanco MA, Celia-Terrassa T, et al. Direct targeting of Sec23a by miR-200s influences cancer cell secretome and promotes metastatic colonization. Nat Med. 2011; 17:1101–8. [PubMed: 21822286]
5. Chou J, Lin JH, Brenot A, Kim JW, Provot S, Werb Z. GATA3 suppresses metastasis and modulates the tumour microenvironment by regulating microRNA-29b expression. Nat Cell Biol. 2013; 15:201–13. [PubMed: 23354167]
6. Hagan JP, O'Neill BL, Stewart CL, Kozlov SV, Croce CM. At least ten genes define the imprinted Dlk1-Dio3 cluster on mouse chromosome 12qF1. PLoS One. 2009; 4:e4352. [PubMed: 19194500]
7. Formosa A, Markert EK, Lena AM, Italiano D, Finazzi-Agro E, Levine AJ, et al. MicroRNAs, miR-154, miR-299-5p, miR-376a, miR-376c, miR-377, miR-381, miR-487b, miR-485-3p, miR-495 and miR-654-3p, mapped to the 14q32.31 locus, regulate proliferation, apoptosis, migration and invasion in metastatic prostate cancer cells. Oncogene. 2013

8. Liu L, Luo GZ, Yang W, Zhao X, Zheng Q, Lv Z, et al. Activation of the imprinted Dlk1-Dio3 region correlates with pluripotency levels of mouse stem cells. J Biol Chem. 2010; 285:19483–90. [PubMed: 20382743]
9. Stadtfeld M, Apostolou E, Akutsu H, Fukuda A, Follett P, Natesan S, et al. Aberrant silencing of imprinted genes on chromosome 12qF1 in mouse induced pluripotent stem cells. Nature. 2010; 465:175–81. [PubMed: 20418860]
10. Haga CL, Phinney DG. MicroRNAs in the imprinted DLK1-DIO3 region repress the epithelial-to-mesenchymal transition by targeting the TWIST1 protein signaling network. J Biol Chem. 2012; 287:42695–707. [PubMed: 23105110]
11. Luk JM, Burchard J, Zhang C, Liu AM, Wong KF, Shek FH, et al. DLK1-DIO3 genomic imprinted microRNA cluster at 14q32. 2 defines a stemlike subtype of hepatocellular carcinoma associated with poor survival. J Biol Chem. 2011; 286:30706–13. [PubMed: 21737452]
12. Nguyen HC, Xie W, Yang M, Hsieh CL, Drouin S, Lee GS, et al. Expression differences of circulating microRNAs in metastatic castration resistant prostate cancer and low-risk, localized prostate cancer. Prostate. 2013; 73:346–54. [PubMed: 22887127]
13. Bryant RJ, Pawlowski T, Catto JW, Marsden G, Vessella RL, Rhees B, et al. Changes in circulating microRNA levels associated with prostate cancer. British journal of cancer. 2012; 106:768–74. [PubMed: 22240788]
14. Cazzoli R, Buttitta F, Di Nicola M, Malatesta S, Marchetti A, Rom WN, et al. microRNAs Derived from Circulating Exosomes as Noninvasive Biomarkers for Screening and Diagnosing Lung Cancer. J Thorac Oncol. 2013; 8:1156–62. [PubMed: 23945385]
15. Xu J, Wang R, Xie ZH, Odero-Marah V, Pathak S, Multani A, et al. Prostate cancer metastasis: role of the host microenvironment in promoting epithelial to mesenchymal transition and increased bone and adrenal gland metastasis. Prostate. 2006; 66:1664–73. [PubMed: 16902972]
16. Hu P, Chu GC, Zhu G, Yang H, Luthringer D, Prins G, et al. Multiplexed quantum dot labeling of activated c-Met signaling in castration-resistant human prostate cancer. PLoS One. 2011; 6:e28670. [PubMed: 22205960]
17. Chu GC, Zhau HE, Wang R, Rogatko A, Feng X, Zayzafoon M, et al. RANK- and c-Met-mediated signal network promotes prostate cancer metastatic colonization. Endocr Relat Cancer. 2014; 21:311–26. [PubMed: 24478054]
18. Josson S, Matsuoka Y, Gururajan M, Nomura T, Huang WC, Yang X, et al. Inhibition of beta2-microglobulin/hemochromatosis enhances radiation sensitivity by induction of iron overload in prostate cancer cells. PLoS One. 2013; 8:e68366. [PubMed: 23874600]
19. Josson S, Sung SY, Lao K, Chung LW, Johnstone PA. Radiation modulation of microRNA in prostate cancer cell lines. Prostate. 2008; 68:1599–606. [PubMed: 18668526]
20. Taylor BS, Schultz N, Hieronymus H, Gopalan A, Xiao Y, Carver BS, et al. Integrative genomic profiling of human prostate cancer. Cancer cell. 2010; 18:11–22. [PubMed: 20579941]
21. Gao J, Aksoy BA, Dogrusoz U, Dresdner G, Gross B, Sumer SO, et al. Integrative analysis of complex cancer genomics and clinical profiles using the cBioPortal. Science signaling. 2013; 6:pl1. [PubMed: 23550210]
22. Nomura T, Huang WC, Zhau HE, Wu D, Xie Z, Mimata H, et al. Beta2-microglobulin promotes the growth of human renal cell carcinoma through the activation of the protein kinase A, cyclic AMP-responsive element-binding protein, and vascular endothelial growth factor axis. Clin Cancer Res. 2006; 12:7294–305. [PubMed: 17189401]
23. Yang X, Shi C, Tong R, Qian W, Zhau HE, Wang R, et al. Near IR heptamethine cyanine dye-mediated cancer imaging. Clin Cancer Res. 2010; 16:2833–44. [PubMed: 20410058]
24. Josson S, Nomura T, Lin JT, Huang WC, Wu D, Zhau HE, et al. beta2-microglobulin induces epithelial to mesenchymal transition and confers cancer lethality and bone metastasis in human cancer cells. Cancer research. 2011; 71:2600–10. [PubMed: 21427356]
25. Zhau HY, Chang SM, Chen BQ, Wang Y, Zhang H, Kao C, et al. Androgen-repressed phenotype in human prostate cancer. Proc Natl Acad Sci U S A. 1996; 93:15152–7. [PubMed: 8986779]
26. Kircher M, Bock C, Paulsen M. Structural conservation versus functional divergence of maternally expressed microRNAs in the Dlk1/Gtl2 imprinting region. BMC Genomics. 2008; 9:346. [PubMed: 18651963]

27. Gonzalez-Nieves R, Desantis AI, Cutler ML. Rsu1 contributes to regulation of cell adhesion and spreading by PINCH1-dependent and - independent mechanisms. J Cell Commun Signal. 2013; 7:279–93. [PubMed: 23765260]

28. Dougherty GW, Jose C, Gimona M, Cutler ML. The Rsu-1-PINCH1-ILK complex is regulated by Ras activation in tumor cells. Eur J Cell Biol. 2008; 87:721–34. [PubMed: 18436335]

29. Becker-Santos DD, Guo Y, Ghaffari M, Vickers ED, Lehman M, Altamirano-Dimas M, et al. Integrin-linked kinase as a target for ERG-mediated invasive properties in prostate cancer models. Carcinogenesis. 2012; 33:2558–67. [PubMed: 23027626]

30. Solomon DA, Kim T, Diaz-Martinez LA, Fair J, Elkahloun AG, Harris BT, et al. Mutational inactivation of STAG2 causes aneuploidy in human cancer. Science. 2011; 333:1039–43. [PubMed: 21852505]

31. Kim MS, Kim SS, Je EM, Yoo NJ, Lee SH. Mutational and expressional analyses of STAG2 gene in solid cancers. Neoplasma. 2012; 59:524–9. [PubMed: 22668012]

32. Gao Y, Wang J, Fan G. NPRL2 is an independent prognostic factor of osteosarcoma. Cancer Biomark. 2013; 12:31–6. [PubMed: 23321467]

33. Senchenko VN, Anedchenko EA, Kondratieva TT, Krasnov GS, Dmitriev AA, Zabarovska VI, et al. Simultaneous down-regulation of tumor suppressor genes RBSP3/CTDSPL, NPRL2/G21 and RASSF1A in primary non-small cell lung cancer. BMC Cancer. 2010; 10:75. [PubMed: 20193080]

34. Ueda K, Kawashima H, Ohtani S, Deng WG, Ravoori M, Bankson J, et al. The 3p21. 3 tumor suppressor NPRL2 plays an important role in cisplatin-induced resistance in human non-small-cell lung cancer cells. Cancer research. 2006; 66:9682–90. [PubMed: 17018626]

Translational Relevance

Currently there are limited options for targeted treatment or biomarker of cancer bone metastasis. In this study, we have identified a novel role for miR-409-3p/-5p, in prostate tumor growth, epithelial to mesenchymal transition, stemness and bone metastasis. miR-409-3p/-5p is located in an embryonically regulated cluster and appears to be activated during metastasis. We demonstrate that both miR-409-3p and miR-409-5p are elevated in tumor tissues of prostate cancer patients with high Gleason score. Using publicly available database we observed that elevated miR-409-3p levels correlate with patient disease free survival. Overexpression of miR-409-3p/-5p in mouse prostate induces tumor growth and inhibition of miR-409-5p results in decreased bone metastasis in experimental models. Thus miR-409-3p/-5p, implicated in embryonic development, has an unexpected oncogenic role in prostate cancer bone metastasis, and thus could serve both as a biomarker and as a therapeutic target.

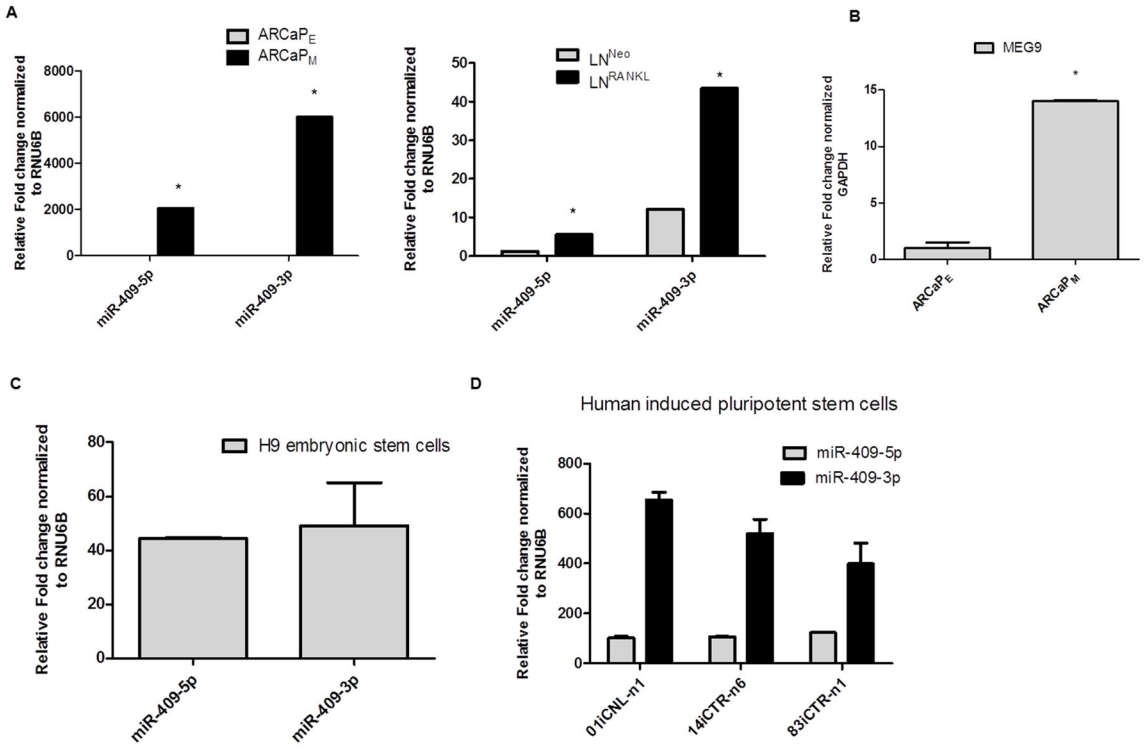

Figure 1.

MicroRNA miR-409-3p/-5p in the imprinted DLK1-DIO3 cluster is overexpressed in bone metastatic EMT models of human PCa. A, miR-409-3p/-5p in bone metastatic PCa models (mesenchymal cells ARCaP$_M$ compared to ARCaP$_E$) and (LNCaP^{Neo} verses LNCaP^{RANKL} PCa cells). All miRNA and RNA analysis was performed by qRT-PCR analysis. B, mRNA levels of MEG9 of ARCaP$_E$ and ARCaP$_M$ PCa cells. C, miR-409-3p/-5p expression in H9 embryonic stem cells and, D, iPSCs. *: $p<0.05$ were considered to be statistically significant by t-test.

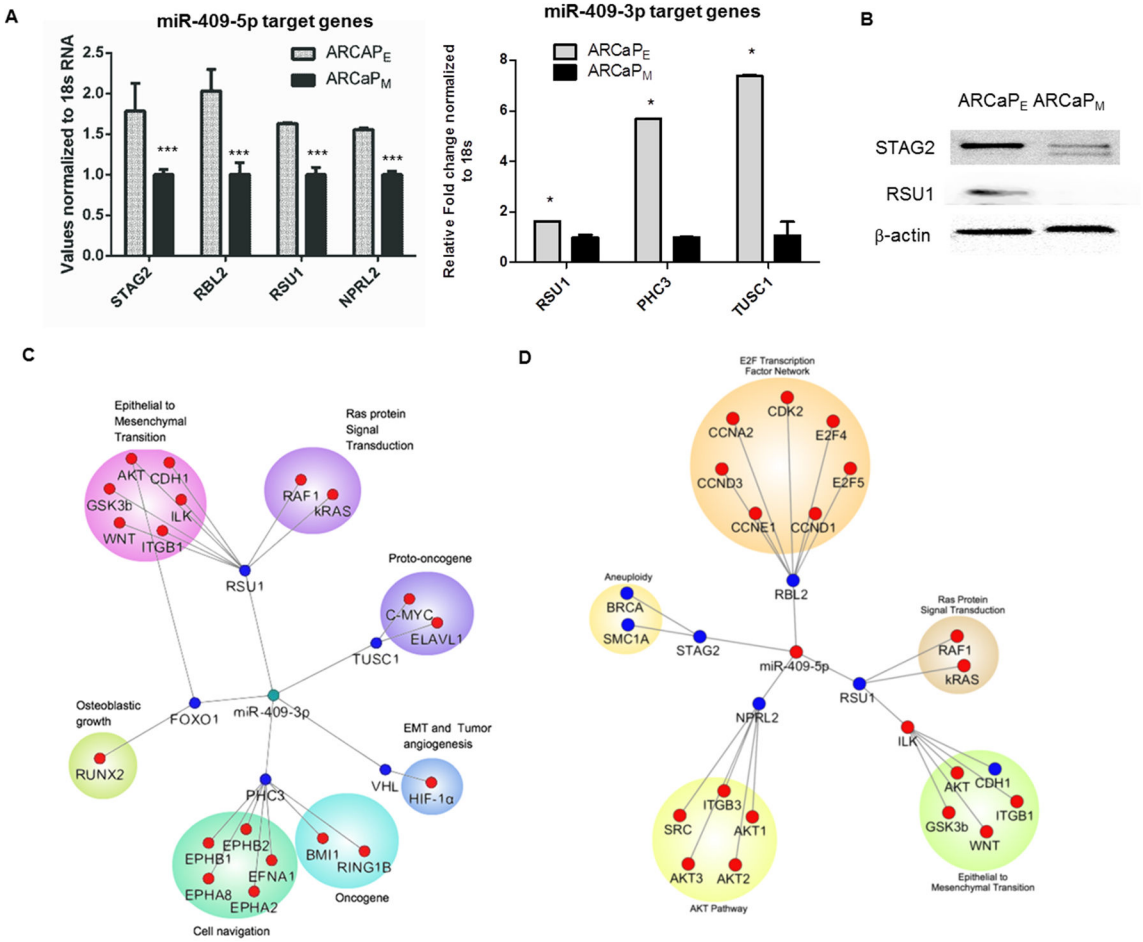

Figure 2.

miR-409 inhibits tumor suppressor genes in prostate cancer. A, mRNA targets of miR-409-5p: STAG2, RBL2, RSU1 and NPRL2 and mRNA targets of miR-409-3p: RSU1, PHC3 and TUSC1, assayed by triplicate wells in qRT-PCR of ARCaP$_E$ and ARCaP$_M$ cells. The representative RT-PCR is shown. The experiment was repeated twice. B, Western analysis of STAG2 and RSU1 in ARCaP$_E$ and ARCaP$_M$ PCa cells. C and D, Cytoscape images of miR-409-3p and miR-409-5p signaling pathways. *: $p<0.05$ were considered to be statistically significant by t-test.

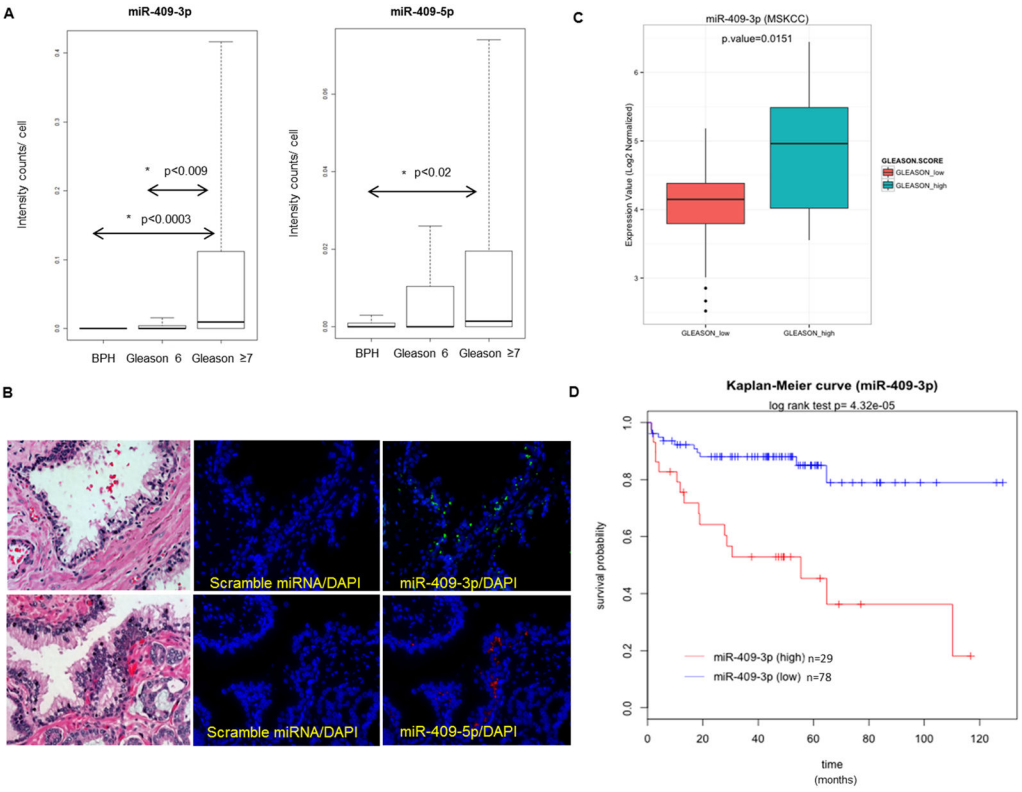

Figure 3.

Human prostatic tissues with higher Gleason score and prostate cancer bone metastasis tissues express elevated levels of miR-409. A, Quantitative analysis of miR-409-3p and miR-409-5p expression in tumor tissues with Gleason grade. B, Representative image of miR-409-3p (green) and miR-409-5p (red) expression in tumor tissues and H&E staining (40x). The tissue array consisted of BPH (N=14), Gleason 6 (N=26) and Gleason ≥ 7 (N=35), data analyzed by Kruskal-Wallis one way analysis of variance- Tukey method. C, miR-409-3p expression in Gleason_high (N=29) and Gleason_low (N=78) based on MSKCC dataset. D, Kaplan-Meier disease free survival (DFS) curves for the prostate cancer patients, based on miR-409-3p expression in the MSKCC dataset. The y-axis is disease free survival probability, and the x-axis is survival in months. Blue line represents the DFS of patients with miR-409-3p lower than the median of the normal individuals (n=78). Red line represents the DFS of patients with miR-409-3p higher than the median of the normal individuals (n=29). Data was analyzed using log-rank test (p=4.3e-05). *: p<0.05 were considered to be statistically significant.

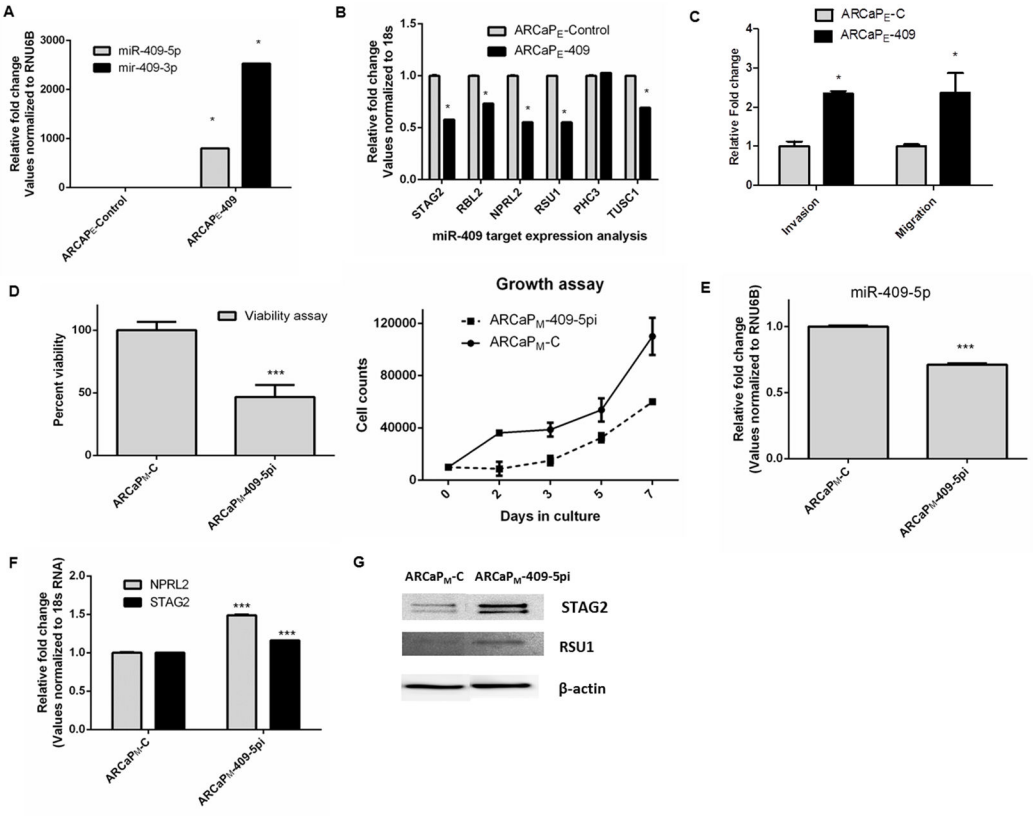

Figure 4.

Ectopic expression of miR-409 leads to increased invasiveness and aggressiveness of prostate cancer cells and conversely inhibition of miR-409 results in increased cell death in PCa cells. A, miR-409-5p and -3p expression by qRT-PCR in $ARCaP_E$-C and $ARCaP_E$-409 expressing PCa cells. B, RNA expression of miR-409-5p/-3p targets in $ARCaP_E$-C and $ARCaP_E$-409 expressing PCa cells assayed by real time PCR. (miR-409-5p mRNA targets: STAG2, RBL2, NPRL2 and RSU1and miR-409-3p mRNA targets: RSU1, PHC3 and TUSC1). C, Invasion and migration assay of in $ARCaP_E$-C and $ARCaP_E$-409 expressing PCa cells. D, Cell viability in $ARCaP_M$ PCa cells in response to a miR-409-5p inhibitor. Growth curve of $ARCaP_M$-C and $ARCaP_M$-409-5pi PCa cells. E, Expression of miR-409-5p assayed by qRT- PCR in $ARCaP_M$-C control PCa and $ARCaP_M$-409-5pi (miR-409-5p inhibitor transfected cells). F, RNA expression of miR-409-5p targets in $ARCaP_M$-C control and $ARCaP_M$-409-5pi cells assayed by qRT- PCR. (miR-409-5p mRNA targets: NPRL2 and STAG2). G, Protein expression of STAG2 and RSU1 in $ARCaP_M$-C cells and $ARCaP_M$-409-5pi cells. *: $p<0.05$ were considered to be statistically significant by t-test.

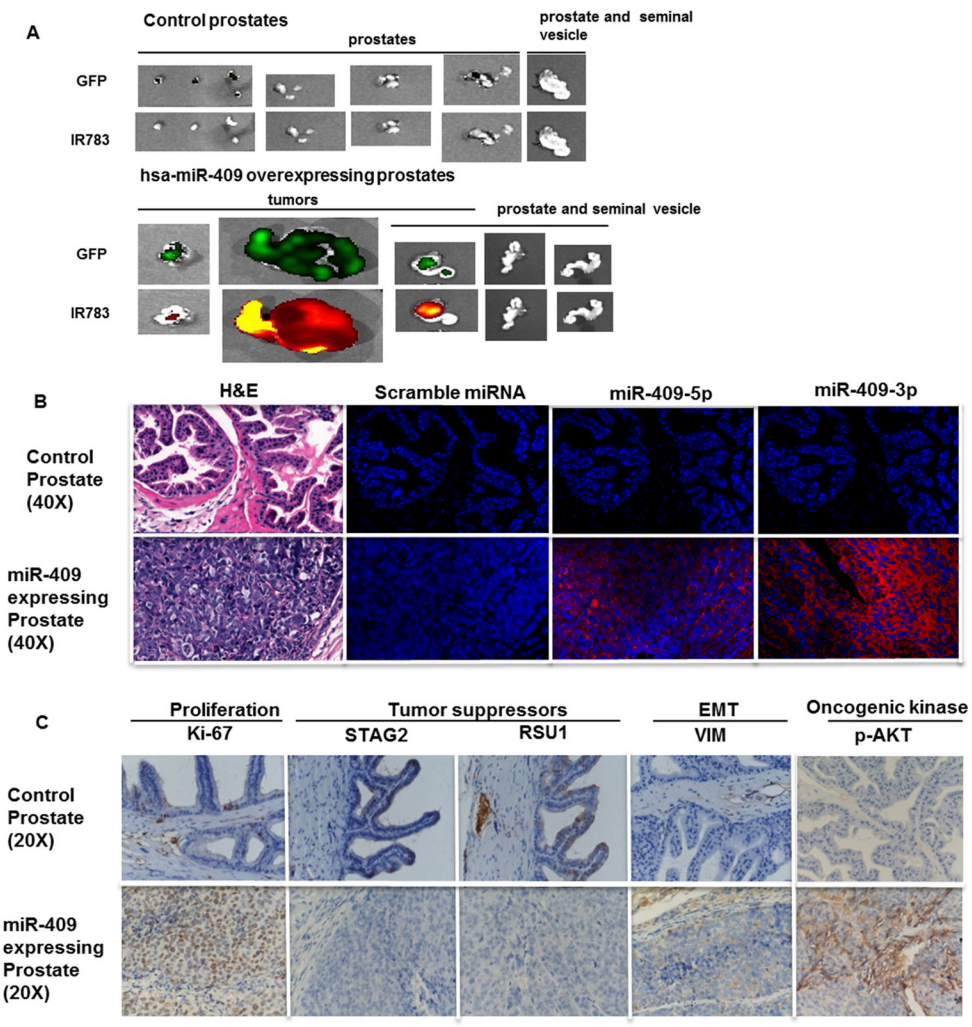

Figure 5.

Ectopic expression of miR-409 in the prostate gland transforms normal prostate epithelia, promotes tumorigenecity, EMT and stemness *in vivo.* A, Comparison of normal prostate and miR-409 expressing prostates. Top row represents green fluorescence for cells containing control GFP plasmid or miR-409 GFP expressing plasmid. Bottom panel represent tumor specific NIR dye (IR783) uptake in control or miR-409 expressing prostates. B, H&E staining of normal control prostate and adenocarcinoma lesions of miR-409 overexpressing prostates (40x), followed by miRNA detection of scramble miRNA and miR-409-5p/-3p of control and miR-409 expressing tissues by ISH and QD detection (40x). C, IHC staining of Ki-67, STAG2, RSU1, vimentin and p-AKT in control prostate and miR-409 expressing prostate tissues (20x).

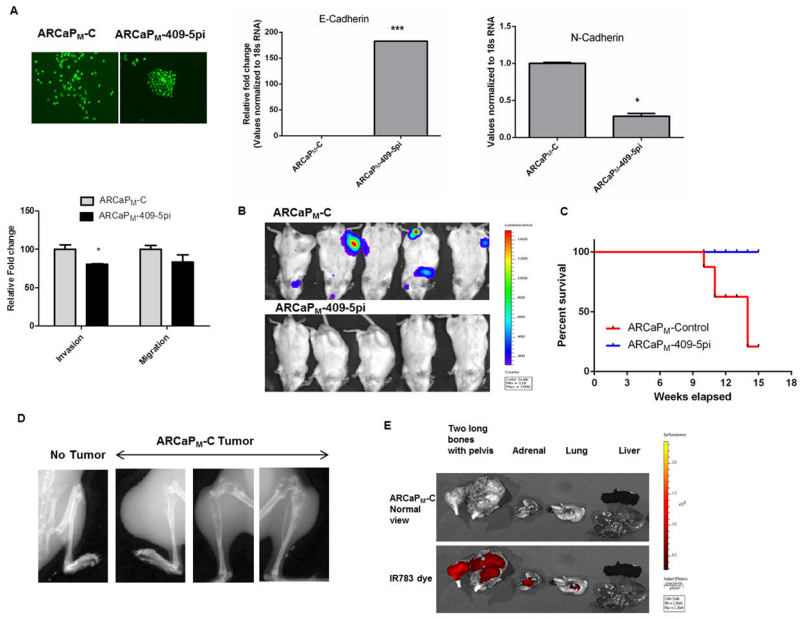

Figure 6.

Inhibition of miR-409-5p results in decreased bone metastasis in PCa *in vivo*. A, Morphological EMT changes in miR-409-5p inhibited $ARCaP_M$ cells; magnification 10x. RNA expression assayed by qRT-PCR of EMT markers, E-cadherin and N-cadherin. Migration and invasion assay of $ARCaP_M$-C and $ARCaP_M$-409-5pi PCa cells (n=3). B, Metastatic lesions observed by luciferase imaging of tumors of $ARCaP_M$–C cells and $ARCaP_M$-409-5pi cells in SCID/Beige mice following intra-cardial injections (N=5). C, Kaplan Meier survival curve of mice injected with $ARCaP_M$–C cells and $ARCaP_M$-409-5pi cells mice. D, X-ray image of metastatic bone lesion from $ARCaP_M$–C bone tumors. E, Tumor dye (IR-783 dye) uptake by $ARCaP_M$–C metastatic tumors from a representative mouse.